Low-lying electronic states of CH_3NO_2 via photoelectron imaging of the nitromethane anion

Daniel J. Goebbert, Kostyantyn Pichugin, and Andrei Sanov[a)]
Department of Chemistry and Biochemistry, University of Arizona, Tucson, Arizona 85721-0041, USA

(Received 6 August 2009; accepted 7 October 2009; published online 30 October 2009)

Negative-ion photoelectron imaging at 532, 392, 355, and 266 nm is used to assign several low-lying electronic states of neutral nitromethane CH_3NO_2 at the geometry corresponding to the anion equilibrium. The observed neutral states include (in the order of increasing binding energy) the $X\ ^1A'$ ground state, two triplet excited states, $a\ ^3A''$ and $b\ ^3A''$, and the first excited singlet state, $A\ ^1A''$. The state assignments are aided by the analysis of the photoelectron angular distributions resulting from electron detachment from the a′ and a″ symmetry molecular orbitals and the results of theoretical calculations. The singlet-triplet ($X\ ^1A'-a\ ^3A''$) splitting in nitromethane is determined as $2.90^{+0.02}_{-0.07}$ eV, while the vibrational structure of the band corresponding to the formation of the $a\ ^3A''$ state of CH_3NO_2 is attributed to the ONO bending and NO_2 wagging motions excited in the photodetachment of the anion. © *2009 American Institute of Physics*. [doi:10.1063/1.3256233]

I. INTRODUCTION

Nitromethane, CH_3NO_2, is the simplest nitrosubstituted organic compound. It serves not only as a solvent, but synthetic reagent and explosive. The nitromethane molecule has a large dipole moment, 3.46 D,[1] which is sufficient for formation of dipole bound anions.[2] This property makes nitromethane attractive for studying gas-phase electron attachment,[3–8] although experimental observation of the dipole bound state has, until recently,[9] remained elusive despite indirect evidence from earlier Rydberg electron transfer experiments.[4] A number of studies have attempted to elucidate the mechanism of electron transfer using free electrons,[10] alkali metal atoms,[3,5–7] or high Rydberg atoms.[4] These studies have shown that nitromethane and nitromethane anion have a number of low-lying electronic states. These states have also been observed by optical absorption and photodissociation,[8,11–13] as well as electron scattering.[3,8,14] However, the assignment of many states has remained ambiguous and discrepancies with theory remain. In this work, we examine and assign several excited states of nitromethane using photoelectron imaging of the nitromethane anion.

Neutral nitromethane has a nearly planar $C-NO_2$ atomic arrangement. Its lowest-unoccupied molecular orbital (LUMO) is a π^* orbital localized primarily on the NO_2 group. It has been suggested that the LUMO acts as a gateway to the valence bound anion state.[4,15] Theory has shown that pyramidalization at the N atom lowers the energy of the π^*-type orbital allowing electron attachment.[6] Accordingly, experiment shows that nitromethane anion is nonplanar[16] and both theory and experiment are in agreement that the excess electron in $CH_3NO_2^-$ occupies the π^* orbital on the nitrogroup.[5]

While much of the experimental knowledge of nitromethane anion comes from electron transfer experiments, several spectroscopic studies have also been carried out.[4,8,9,16] Early negative-ion photoelectron spectra of the anion showed a broad band at low electron binding energies.[4] The threshold for photodetachment was assigned to the first peak in the photoelectron band at 0.26 ± 0.08 eV. This work was later followed by infrared spectroscopy studies which demonstrated that vibrational excitation of the CH stretches of $CH_3NO_2^-$ resulted in autodetachment.[16,17] More recently, this method has been enhanced by combining infrared excitation with photoelectron imaging detection of the slow electrons from autodetachment.[9] By utilizing high level *ab initio* calculations and a Franck–Condon simulation to fit the experimental spectrum, the adiabatic electron affinity of CH_3NO_2 was reassigned as 0.172 ± 0.006 eV. The high resolution autodetachment spectrum also revealed a weak low energy feature which has been tentatively assigned to detachment of a dipole-bound electron.[9]

Concerning the excited states of nitromethane, electron energy loss measurements reported a low-energy triplet at around 3.8 eV,[14] while an excited singlet state was reported near 4.3 eV.[18,19] Optical absorption spectroscopy shows an intense band centered at 6.25 eV, with a weaker feature at 4.5 eV, both transitions are assigned to excited singlet states.[8] Photodissociation of nitromethane via optical excitation to excited singlet states has been studied for decades, and yet a complete understanding of the dissociation mechanism and the electronic states involved has not been reached.[11–13]

Due to the interesting photochemistry and electron capture dynamics of nitromethane, many theoretical studies on the neutral and radical anion have been carried out.[20–25] Several early theoretical investigations of the excited states of the neutral reported low energy triplet states, with slightly higher energy singlet states. The energies from these modest calculations are qualitative at best, and agreement with the electron transfer studies is mixed.[20–22] Modern *ab initio* methods have been used to study the excited states of ni-

a)Author to whom correspondence should be addressed. Electronic mail: sanov@u.arizona.edu.

TABLE I. Energies of excited electronic states of nitromethane relative to the $X\ ^1A'$ ground state.

State[a]	Energy (eV)	Method	Ref.
$a\ ^3A''$	3.01	Theory[b]	20
	3.13	Theory[c]	21
	3.75	Theory[d]	23
	3.5	MB[e]	18
	3.8	EEL[f]	14
$b\ ^3A''$	4.60	Theory[b]	20
	3.78	Theory[d]	23
$c\ ^3A'$	3.71	Theory[b]	20
	4.11	Theory[d]	23
$A\ ^1A''$	4.56	Theory[b]	20
	3.86	Theory[c]	21
	4.22	Theory[h]	22
	3.97	Theory[d]	23
	4.3	MB[e]	18
	4.3	EEL[f]	19
	4.25	EEL[g]	8
$B\ ^1A'$	4.41	Theory[b]	20
	3.41	Theory[c]	21
	4.58	Theory[h]	22
	4.29	Theory[d]	23
	4.5	VUV[g]	8
	4.45	EEL[f]	14
$C\ ^1A''$	5.8	Theory[b]	20
	6.43	Theory[c]	21
	6.63	Theory[h]	22
	6.15	Theory[d]	23
	6.25	VUV[g]	8
	6.23	EEL[f]	14
	6.1	EEL[f]	19
	6.23	EEL[f]	8
	6.5	MB[e]	18

[a]The italicized state labels used throughout this work are based on the energetic state ordering expected for the neutral ground-state geometry.
[b]Semiempirical extended Hückel.
[c]CNDO/s-CI.
[d]CASPT2.
[e]Molecular beam collisions.
[f]Electron energy loss spectroscopy.
[g]Vacuum ultraviolet absorption spectroscopy.
[h]SCF-CI.

tromethane in relation to its photodissociation.[23–25] In particular, a recent study using the complete active space self-consistent-field procedure with second-order perturbation theory (CASPT2) and the ANO-L basis set identified a number of excited states of nitromethane at various geometries.[23] A summary of some of the previously assigned low-energy electronic states and their relative energies are listed in Table I. The A' and A'' state labeling in Table I and throughout the paper refers to reflection symmetry with respect to the HCN plane bisecting the ONO bond angle. The italicized state labels in Table I are intended to follow the usual spectroscopic convention, reflecting the corresponding state ordering at the geometry of neutral nitromethane. However, because of the spreads in the state energies derived from different experiments and theoretical predictions, the state label assignments in Table I are somewhat uncertain in some cases, particularly so for the $b\ ^3A''$ and $c\ ^3A'$ states. These states have been studied only theoretically and we chose the relative CASPT2 energies to determine their energetic order. It should also be emphasized that the state ordering at the anion geometry can be drastically different.

Several observations stemming from the wide range of entries in Table I are particularly worth noting. First, the excited singlet states have been most extensively studied, and agreement with theory and experiment is reasonable for most assignments. Second, there are few reported experimental observations of excited triplet states. Characterization of these states is important, as they have been proposed to play roles in the photodissociation of nitromethane,[23] but they cannot be detected by direct absorption spectroscopy because of the spin selection rule.

Negative-ion photoelectron spectroscopy has no such limitation. In the present study, we use photoelectron imaging to examine $CH_3NO_2^-$ photodetachment at 532, 392, 355, and 266 nm. We find that at least three low lying excited electronic states of nitromethane are accessible with 266 nm photons. The symmetries of the observed excited states of nitromethane are assigned by analyzing the photoelectron angular distributions (PADs) with the aid of theoretical calculations.

II. EXPERIMENTAL ARRANGEMENT

The experiments were carried out on a pulsed dual time-of-flight (TOF) mass-spectrometer equipped with a velocity-map[26] imaging assembly for detecting photoelectrons. The instrument has been described in detail previously.[27] Nitromethane vapor in Ar carrier gas was introduced into a high vacuum chamber through a pulsed General Valve (Series 99) nozzle operating at a 50 Hz repetition rate and 30 psi backing pressure. The anions are formed by secondary-electron attachment following collisions with high-energy electrons (1 keV) from an electron gun.[28] The resulting anions are mass-selected using the primary TOF spectrometer. In the velocity-map imaging region, the ion beam is intersected at a right angle with a pulsed linearly polarized laser beam timed to overlap only with the ions of interest. In this work, we use the frequency-doubled (532 nm), tripled (355 nm), or quadrupled (266 nm) output from a pulsed Nd:YAG (yttrium aluminum garnet) laser (Spectra Physics, Inc., Lab-50 model with pulse energies 10, 3.5, and 0.07 mJ, respectively). The 392 nm radiation (0.2 mJ and 100 fs pulses) is generated as the second harmonic of an amplified Ti:sapphire laser system (Spectra Physics, Inc.).

The velocity-map imaging assembly is based on the design by Eppink and Parker.[26] The laser radiation is polarized linearly, parallel to the plane of the imaging detector. Photoelectrons are accelerated using an electrostatic lens and focused onto a position-sensitive microchannel plate detector fiber-optically coupled to a phosphor screen. A 1.0 Mpixel camera records the photoelectron images. The reported images represent 10^4–10^5 experimental cycles each. The three-dimensional photoelectron velocity distributions are reconstructed form the images by the inverse Abel transformation using the BASEX program.[29] Integration of a transformed image over the angular domain gives the photoelectron spec-

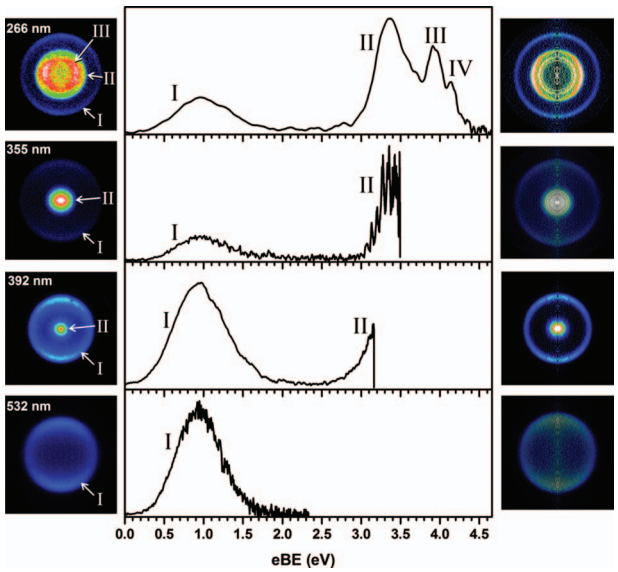

FIG. 1. Raw (left) and Abel-inverted (right) photoelectron images of nitromethane anion at 266, 355, 392, and 532 nm, shown on varying velocity scales. The laser polarization axis is vertical in the plane of the figure. (Center) Photoelectron spectra obtained from the images.

trum, while integration over the radial coordinate yields the PAD. The PADs are fit using the equation

$$I(\theta) = (\sigma/4\pi)[1 + \beta P_2(\cos\ \theta)], \quad (1)$$

to determine the anisotropy parameter β.[30,31] In Eq. (1), σ is the total photodetachment cross section, $P_2(\cos\ \theta)$ is the second-order Legendre polynomial, and θ is the electron emission angle with respect to the laboratory-frame laser polarization axis (z).

Density functional theory (DFT) calculations were carried out using the GAUSSIAN 03 program at the B3LYP/aug-cc-pVDZ level.[32] Geometry optimizations and frequencies were calculated for the ground states of the anion, neutral and first excited triplet state, which was also explored at the fixed equilibrium geometry of the anion.

III. RESULTS

A. Photoelectron images and spectra

The raw and Abel transformed photoelectron images obtained at 532, 392, 355, and 266 nm, as well as the corresponding photoelectron spectra, are shown in Fig. 1. The images were recorded at different velocity-mapping potentials and their apparent sizes cannot be compared directly. For quantitative comparison, the spectra are plotted versus electron binding energy (eBE), calculated by subtracting the electron kinetic energy (eKE) from the photon energy.

All photoelectron images in Fig. 1 show the outer band labeled with the Roman numeral I. The corresponding angular distributions peak in the direction parallel to the laser polarization axis (vertical in the figure plane). In the corresponding spectra, the broad and unstructured band I peaks at eBE=0.96 eV, which is consistent with the previous determinations of the vertical detachment energy (VDE) of the lowest photodetachment transition in $CH_3NO_2^-$.[4,9]

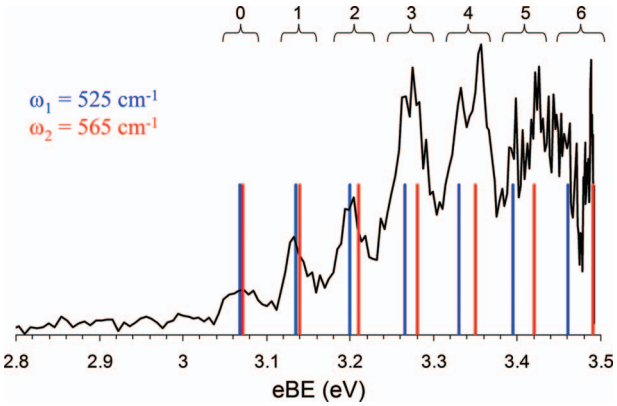

FIG. 2. Band II in the 355 nm photoelectron spectrum of $CH_3NO_2^-$ from Fig. 1, showing details of its vibrational structure and individual peak labels (0–6). Superimposed with the experimental spectrum are the stick spectra for two vibrational progressions with the common origin at eBE=3.07 eV and frequencies ω_1=525 cm^{-1} and ω_2=565 cm^{-1} (no anharmonicity or combination bands are included).

The 392 nm photoelectron image shows the onset of another feature near the image center; band II, which is also seen at 355 and 266 nm. The 355 nm spectrum reveals partially resolved vibrational structure within band II. This structure is expanded in Fig. 2, which shows a portion of the 355 nm spectrum corresponding to the spectral range of band II. The partially resolved peaks comprising band II are labeled with 0–6, in accordance with the corresponding vibrational quantum numbers, whose assignment is discussed in Sec. IV D. We assign the band origin to the first peak rising above the noise level (peak 0), but stress that this assignment is not unambiguous, as is often the case for photodetachment transitions involving a significant geometry change. The assigned origin transition is centered at eBE=3.07 eV, while the maximum of the overall band II is at 3.36 eV, as determined from the 266 nm spectrum in Fig. 1. The vibrational structure of band II is washed out at 266 nm due to the decreasing absolute energy resolution afforded by photoelectron imaging at increasing eKEs.

Finally, the 266 nm image and spectrum in Fig. 1 show the two abovementioned bands, I and II, plus two additional features, III and IV, peaking at eBE=3.91 and 4.12 eV, respectively. Bands II, III, and IV exhibit angular distributions peaking in the direction perpendicular to the laser polarization axis, in contrast to band I. The photoelectron anisotropy parameters, obtained by least-squares fits to the model function in Eq. (1) are listed in Table II, along with the electron kinetic and binding energies determined for the observed transitions at each wavelength. For 355 nm, the angular distributions for individual peaks II_0–II_5 are reported along with the PAD for the entire band II.

B. Theory results

To aid in the analysis of the experimental data, the structural features of the $CH_3NO_2^-$ anion and the CH_3NO_2 neutral molecule in the ground ($X\ ^1A'$) and first excited ($a\ ^3A''$) electronic states were examined using DFT at the B3LYP/aug-cc-pVDZ level. For the ground state, the results of these calculations in general agreement with the higher-level com-

TABLE II. Nitromethane photoelectron features, binding energies, and anisotropies (β) as measured at different photon energies.

Band[a]	Wavelength (nm)	Transition eBE or VDE (eV)[b]	β [c]	Neutral state assignment
I	532	0.95	0.56	$X\ ^1A'$
	392	0.97	0.45	
	355	0.95	0.39	
	266	0.96	0.39	
II	355	3.36	−0.16	$a\ ^3A''$
	266	3.36	−0.34	
II_0	355	3.07	−0.27	v=0 [d]
II_1	355	3.13	−0.28	v=1
II_2	355	3.20	−0.25	v=2
II_3	355	3.28	−0.22	v=3
II_4	355	[e]	−0.19	v=4
II_5	355	[e]	−0.11	v=5
III	266	3.91	−0.21	$b\ ^3A''$
IV	266	4.12	−0.16	$A\ ^1A''$

[a]The band labels are defined in Fig. 1. The subscripts distinguishing the individual peaks comprising band II correspond to the numerical labels assigned to these transitions in Fig. 2.
[b]VDE or eBE for the band maximum. Uncertainty ±0.01 eV.
[c]Uncertainty ±0.07.
[d]Vibrational quantum numbers (v) correspond to the ONO bending mode or NO_2 wagging mode in CH_3NO_2, as discussed in Sec. IV D.
[e]See Fig. 2.

putations by Weber and co-workers.[9] We focus primarily on the B3LYP results, which enable consistent comparison of different electronic states while being less demanding computationally.

The optimized structures with important geometrical parameters are shown in Fig. 3. In the anion, the plane of the NO_2 group is angled relative to the CN bond, in contrast to the nearly planar C–NO_2 arrangement for the ground-state neutral. The calculated adiabatic electron affinity of CH_3NO_2 (including the zero-point vibrational energy correction) is

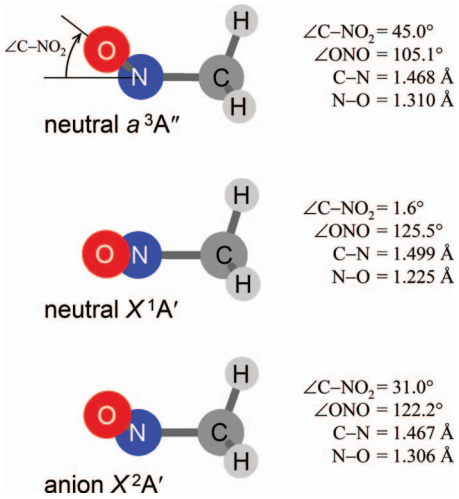

FIG. 3. Equilibrium geometries of nitromethane anion, $CH_3NO_2^-$ ($^2A'$), the ground state of neutral CH_3NO_2 ($X\ ^1A'$), and the lowest-energy excited state of CH_3NO_2 ($a\ ^3A''$), optimized at the B3LYP/aug-cc-pVDZ level of theory.

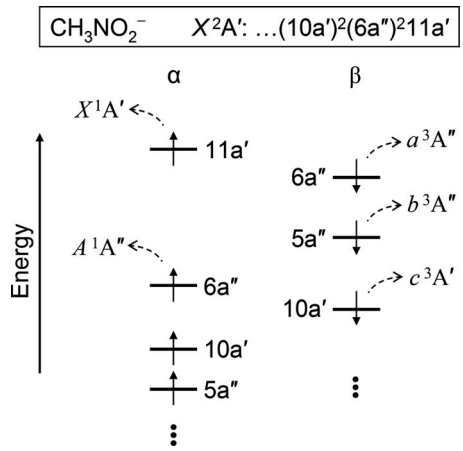

FIG. 4. Electronic structure of $CH_3NO_2^-$ ($^2A'$) as predicted at the UB3LYP/aug-cc-pVDZ level of theory. The symmetries and energetic ordering of the unrestricted α and β spin-orbitals are shown, along with the electronic states of the neutral resulting from removal of the specified electrons (disregarding any relaxation effects).

0.41 eV, compared with the experimentally determined value of 0.172 ± 0.006 eV.[9] The VDE of $CH_3NO_2^-$ is 1.18 eV, compared with the approximately 0.95 eV experimental value determined here and elsewhere.[4] Thus, the B3LYP calculations tend to overestimate, within reasonable limits (<0.25 eV), both the adiabatic and vertical detachment energies of the anion.

The calculated adiabatic eBE of the lowest-energy triplet ($a\ ^3A''$) nitromethane is 2.93 eV, while the anion VDE corresponding to the formation of the $a\ ^3A''$ neutral state is 3.24 eV. These values are in good agreement with the experimental observations summarized in Table II: II_0=3.07 eV and VDE(II)=3.36 eV. The optimized geometry of ($a\ ^3A''$), is qualitatively similar to that of the anion (see Fig. 3), but two geometric parameters do experience significant changes upon photodetachment. These are in the ONO bond angle and the NO_2 wag angle (∠C–NO_2), which change by an estimated 17° and 14°, respectively, between the anion and $a\ ^3A''$ neutral equilibria. Therefore, both the ONO bending and NO_2 wagging vibrational modes should be excited in the $X\ ^2A' \rightarrow a\ ^3A''$ photodetachment transition.

In the absence of previous spectroscopic determinations of these mode frequencies for the $a\ ^3A''$ state of CH_3NO_2, the B3LYP/aug-cc-pVDZ calculations predict (unscaled) harmonic frequencies of 524 cm^{-1} for the ONO bend and 436 cm^{-1} for the NO_2 wag. Similar calculations with the 6-311++G (3df,3pd) basis set give slightly larger values of 547 and 467 cm^{-1}, respectively. For comparison, the B3LYP/aug-cc-pVDZ calculations for the $X\ ^1A'$ state predict 659 and 609 cm^{-1}, respectively, in very good agreement with experiment: the ONO bending frequency in the ground state of nitromethane has been determined to be 657 cm^{-1},[33] while the corresponding frequency for the NO_2 wagging motion is 603 cm^{-1} (according to Gorse *et al.*),[33] 613 ± 56 cm^{-1} (Weber and co-workers),[9] or 645 ± 70 cm^{-1} (Compton *et al.*).[4]

Figure 4 shows a qualitative orbital ordering and occupancy diagram for the ground ($X\ ^2A'$) electronic state of nitromethane anion derived from the spin-unrestricted DFT

calculations. The highest-occupied spin-orbital (α-HOMO) (HOMO denotes highest occupied molecular orbital) of the anion ($11a'\alpha$) is of a′ symmetry, while the next three highest-energy spin-orbitals ($6a''\beta$, $6a''\alpha$, and $5a''\beta$) are all a″. Also indicated in Fig. 4 are the ground and first four excited electronic states of neutral nitromethane, resulting from electron removal from the specified anion spin-orbitals, discounting any geometry or electron relaxation. With a Koopmans' theorem[34] approach, Fig. 4 suggests the following state ordering for neutral nitromethane *at the anion geometry*: $X\ ^1A', a\ ^3A'', b\ ^3A'', A\ ^1A'', c\ ^3A', \ldots$. This order generally agrees with the summary in Table I with the exception of the relative placement of the *A* and *c* states. The discrepancy may stem from the geometry difference between the anion and neutral equilibria, as our calculations are for the anion geometry, while Table I lists state energies relative to the neutral ground state equilibrium.

IV. DISCUSSION

A. Interpretation of the photoelectron angular distributions

PADs are related to the symmetry of the parent orbital from which photoelectrons originate.[31,35–38] Rigorous theoretical prediction of the PADs is in general a complicated task, requiring the calculation of orientation-averaged transition dipole moment matrix elements.[37,38] Qualitative insight can be derived from simpler symmetry-based approaches. One such approach (the $s\&p$ model)[36,39] is based on the following approximations. (1) The expansion of the outgoing photoelectron wave function is restricted to *s* and *p* partial waves only. (2) The orientation averaging is accounted for by considering only three "principal" orientations of the anion with a chosen molecule-fixed axis aligned along the *x*, *y*, and *z* laboratory-frame axes. 3) The allowed characters of emitted partial waves (s,p_x,p_y,p_z) are determined by inspecting the corresponding transition dipole moment matrix element for each of the principal orientations. Owing to the qualitative nature of the model, it is only necessary to identify the nonzero matrix elements, which is easily done using group theory.

Owing to the low symmetry of nitromethane anion (C_s point group), the details of the symmetry analysis in the present case are particularly straightforward and omitted here.[36,39] Predominantly parallel ($\beta>0$) angular distributions are generally expected in detachment from a′ orbitals, as a partial case of detachment from totally symmetric (with respect to the symmetry operations of the corresponding point group) molecular orbitals.[39] Specifically, if restricted to *s* and *p* waves only, the free-electron wave function resulting from detachment from an a′ orbital may consist of *s* waves and two types of *p* waves: one parallel and one perpendicular to the laser polarization direction. Although the exact PAD depends on the matrix-element integrals, such partial-wave combination will tend to yield a predominantly parallel PAD. (All three types of *p* waves, p_x, p_y, and p_z, are needed for an isotropic angular distribution. Removal of one perpendicular *p* wave will bias the distribution along the polarization axis.) Similarly, in detachment from an a″ orbital, only the *p* waves perpendicular to the laser polarization direction are allowed, in addition to *s* waves, yielding a predominantly perpendicular ($\beta<0$) angular distribution.

These predictions, in conjunction with the experimental photoelectron anisotropy parameters in Table II, aid in assignment of the peaks in the photoelectron spectra. Band I in Fig. 1, which exhibits a parallel PAD, is attributed to detachment from an a′ orbital. This assignment is consistent with the predicted symmetry of the anion HOMO ($11a'\alpha$) (see Fig. 4) and hence this band corresponds to the $X\ ^1A'$ state of the neutral. The next three bands in the photoelectron spectra (II–IV) all correspond to $\beta<0$ and should therefore be assigned to detachment from a″ orbitals. This conclusion agrees with the symmetries of the next three energetically lower $CH_3NO_2^-$ spin-orbitals: $6a''\beta$, $6a''\alpha$, and $5a''\beta$ (see Fig. 4). The next two lower-energy spin-orbitals are of the a′ symmetry and one expects their detachment to yield parallel PADs. Since no additional features are observed in the photoelectron images, we conclude that these channels are not accessible with 266 nm and longer-wavelength photons.

B. Electronic states of neutral nitromethane at the anion geometry

While the assignment of band I to the ground state of nitromethane ($X\ ^1A'$) is straightforward based on the previous studies of this system,[4,9] the remaining state assignments are made here for the first time. Assuming the electronic states of the neutral correlate with electron detachment from the corresponding orbitals, we assign band II to the $a\ ^3A''$ state, band III to the $b\ ^3A''$ state, and band IV to the $A\ ^1A''$ state. These assignments are summarized in Table II.

Comparing our assignments to the states in Table I, we find agreement with the predicted state ordering with the exception of the $c\ ^3A'$ state, which is not assigned to any of the features in the present photoelectron images and spectra. Since the $c\ ^3A'$ state would result from photodetachment from an a′ orbital, a parallel PAD is expected, but no such features are observed in the images and spectra at large eBEs. This is not surprising, considering that here we access the excited states via vertical transitions at the anion geometry, while the previous studies of nitromethane summarized in Table I were carried out relative to the neutral ground state. The large geometry difference between the anion $X\ ^2A'$ and neutral $X\ ^1A'$ states (see Fig. 3) could result in a different state ordering and thus explain the absence of the $c\ ^3A'$ state in the photoelectron spectra in Fig. 1. We must, however, cautiously acknowledge that the high-energy features in the 266 nm spectrum in Fig. 1 are broad and overlapping, so a low intensity feature attributable to the $c\ ^3A'$ state might be obscured by the other bands.

C. The singlet-triplet splitting in neutral nitromethane

The drastic geometry difference between the anion and neutral (see Fig. 3) results in the extended vibrational progression in the lowest-energy photodetachment transition for $CH_3NO_2^-$.[4,9] (This progression, corresponding to band I in Fig. 1, is not resolved in the present work.) While the uncertainty in assignment of this band's origin makes the determi-

nation of adiabatic electron affinity of CH_3NO_2 difficult, Weber and co-workers recently reported its very precise measurement, EA=0.172±0.006 eV.[9]

The equilibrium geometry difference between the anion and the lowest-energy triplet state of CH_3NO_2 (the $a\ ^3A''$ state) is less pronounced, but the assignment of the corresponding band origin is still not quite straightforward. We assign II_0 (peak 0 in Fig. 2) as the transition origin with the corresponding eBE of 3.07±0.01 eV. However, for the singlet-triplet energy splitting calculation, we must account for the possibility that the real 0-0 transition might correspond to the weak, not rising above the noise level, feature at 3.00 eV. Thus, we expand the uncertainty range for the origin transition on the lower-energy side to encompass this ambiguous feature and take the adiabatic eBE of triplet nitromethane to be $3.07+^{0.01}/_{-0.07}$ eV. From this result and the above experimentally determined value of electron affinity of singlet CH_3NO_2, the singlet-triplet splitting in nitromethane is calculated as $2.90+^{0.02}/_{-0.07}$ eV.

D. Vibrational progression in lowest-triplet nitromethane

The 355 nm spectrum in Fig. 1 shows partially resolved vibrational structure for band II, corresponding to the $X\ ^2A' \rightarrow a\ ^3A''$ photodetachment transition. Examining the expanded spectrum of this band in Fig. 2, we note that at its low-energy onset the observed structure can be described as an evenly spaced progression of peaks (0–3) with an average spacing of approximately 560 cm^{-1}. The higher energy peaks (4–6) appear to broaden and split, suggesting additional underlying structure due to more than one vibrational mode excited in the photodetachment.

As seen in Fig. 2, the main geometry differences between the anion and the lowest triplet state of CH_3NO_2 are in the ONO bond angle (∠ONO) and the NO_2 wag angle (∠C–NO_2). Vibrations with respect to both of these angles should be excited in photodetachment and considering the magnitudes of the predicted changes (17° and 14°, respectively), one expects both modes to participate to roughly similar extents. This expectation is amplified considering that the predicted frequencies of the ONO bending and NO_2 wagging motions (see Sec. III B), while not degenerate, are both consistent with the observed spacing between the peaks in the photoelectron spectrum. Therefore, accounting for the experimental broadening, the vibrational progressions in both modes will overlap for small numbers of excitation quanta, eventually broadening and splitting the observed peaks as the excitation increases.

To show that the above explanation is consistent with the experiment, Fig. 2 includes stick spectra for two vibrational progressions with the common origin at eBE=3.07 eV and frequencies ω_1=525 cm^{-1} and ω_2=565 cm^{-1} (no anharmonicity or combination bands are included). As the quantum numbers increase, the lines corresponding to the two progressions appear close together initially, but eventually become more separated. (Anharmonicity and combination bands may contribute additional spectral structure). Although the model frequencies ω_1=525 cm^{-1} and ω_2=565 cm^{-1} differ from the B3LYP predictions of 436 and 524 cm^{-1} (aug-cc-pVDZ basis) or 467 and 547 cm^{-1} [6-311++G(3df,3pd)], the discrepancy is not surprising considering the challenging nature of excited-state calculations. The model spectrum nonetheless captures all principal features of the experimentally observed structure. We therefore conclude that the spectral structure is indeed due to the contributions of at least two vibrational modes excited in the photodetachment, most likely the ONO bending and the NO_2 wagging vibrations.

V. CONCLUSIONS

We reported an experimental observation of several low-lying excited states of nitromethane using photoelectron imaging spectroscopy of nitromethane anion. The PADs aid in assignment of the symmetries of the observed electronic states. Namely, opposite-sign photoelectron anisotropy parameters are determined for electron detachment from a′ and a″ molecular orbitals. Using a group theoretical approach, aided by the results of DFT calculations, the observed transitions are assigned (in the order of increasing binding energy) to the $X\ ^1A'$, $a\ ^3A''$, $b\ ^3A''$, and $A\ ^1A''$ electronic states of neutral nitromethane at the anion geometry. The singlet-triplet ($X\ ^1A'$-$a\ ^3A''$) splitting is determined to be $2.90+^{0.02}/_{-0.07}$ eV, while the vibrational structure of the band corresponding to the formation of the lowest triplet state is attributed to the ONO bending and NO_2 wagging vibrations excited in the photodetachment.

ACKNOWLEDGMENTS

We would like to thank Professor J. M. Weber (University of Colorado, Boulder) for his comments on a draft of this paper. This work is supported by the National Science Foundation (Grant No. CHE-0713880).

[1] R. D. J. Nelson, D. R. J. Lide, and A. A. Maryott, Natl. Stand. Ref. Data Ser. (U.S., Natl. Bur. Stand.) 10 (1967).
[2] C. Desfrancois, H. Abdoul-Carime, and J. P. Schermann, Int. J. Mod. Phys. B **10**, 1339 (1996).
[3] R. F. M. Lobo, A. M. C. Moutinho, K. Lacmann, and J. Los, J. Chem. Phys. **95**, 166 (1991).
[4] R. N. Compton, H. S. Carman, C. Desfrancois, H. Abdoulcarmine, J. P. Schermann, J. H. Hendricks, S. A. Lyapustina, and K. H. Bowen, J. Chem. Phys. **105**, 3472 (1996).
[5] P. R. Brooks, P. W. Harland, and C. E. Redden, J. Am. Chem. Soc. **128**, 4773 (2006).
[6] P. R. Brooks, P. W. Harland, and C. E. Redden, J. Phys. Chem. A **110**, 4697 (2006).
[7] P. R. Brooks, P. W. Harland, S. A. Harris, T. Kennair, C. Redden, and J. F. Tate, J. Am. Chem. Soc. **129**, 15572 (2007).
[8] I. C. Walker and M. A. D. Fluendy, Int. J. Mass Spectrom. **205**, 171 (2001).
[9] C. L. Adams, H. Schneider, K. M. Ervin, and J. M. Weber, J. Chem. Phys. **130**, 074307 (2009).
[10] E. Alizadeh, F. Ferreira da Silva, F. Zappa, A. Mauracher, M. Probst, S. Denfil, B. A. T. D. Maerk, P. Limao-Viera, and P. Scheier, Int. J. Mass Spectrom. **271**, 15 (2008).
[11] L. J. Butler, D. Krajnovich, Y. T. Lee, G. Ondrey, and R. Bersohn, J. Chem. Phys. **79**, 1708 (1983).
[12] H. S. Kwok, G. Z. He, R. K. Sparks, and Y. T. Lee, Int. J. Chem. Kinet. **13**, 1125 (1981).
[13] Y. Q. Guo, A. Bhattacharya, and E. R. Bernstein, J. Phys. Chem. A **113**, 85 (2009).
[14] W. M. Flicker, O. A. Mosher, and A. Kupperman, J. Chem. Phys. **72**,

2788 (1980).
[15] T. Sommerfeld, Phys. Chem. Chem. Phys. **4**, 2511 (2002).
[16] J. M. Weber, W. H. Robertson, and M. A. Johnson, J. Chem. Phys. **115**, 10718 (2001).
[17] H. Schneider, K. M. Vogelhuber, F. Schinle, J. F. Stanton, and J. M. Weber, J. Phys. Chem. A **112**, 7498 (2008).
[18] M. A. D. Fluendy and S. Lunt, Mol. Phys. **49**, 1007 (1983).
[19] T. McAllister, J. Chem. Phys. **57**, 3353 (1972).
[20] K. L. McEwen, J. Chem. Phys. **32**, 1801 (1960).
[21] L. E. Harris, J. Chem. Phys. **58**, 5615 (1973).
[22] C. Mijoule, S. Odiot, S. Fliszar, and J. M. Schnur, J. Mol. Struct.: THEOCHEM, **149**, 311 (1987).
[23] J. F. Arenas, J. C. Otero, D. Pelaez, and J. Soto, J. Chem. Phys. **122**, 084324 (2005).
[24] J. F. Arenas, J. C. Otero, D. Pelaez, J. Soto, and L. Serrano-Andres, J. Chem. Phys. **121**, 4127 (2004).
[25] J. F. Arenas, J. C. Otero, D. Pelaez, and J. Soto, J. Chem. Phys. **119**, 7814 (2003).
[26] A. Eppink and D. H. Parker, Rev. Sci. Instrum. **68**, 3477 (1997).
[27] L. Velarde, T. Habteyes, and A. Sanov, J. Chem. Phys. **125**, 114303 (2006).
[28] M. A. Johnson and W. C. Lineberger, in *Techniques for the Study of Ion Molecule Reactions*, edited by J. M. Farrar and W. H. Saunders (Wiley, New York, 1988), p. 591.
[29] V. Dribinski, A. Ossadtchi, V. A. Mandelshtam, and H. Reisler, Rev. Sci. Instrum. **73**, 2634 (2002).
[30] C. N. Yang, Phys. Rev. **74**, 764 (1948).
[31] J. Cooper and R. N. Zare, in *Atomic Collision Processes*, edited by S. Geltman, K. T. Mahanthappa, and W. E. Brittin (Gordon and Breach, New York, 1968), Vol. XI-C, p. 317.
[32] M. J. Frisch, G. W. Trucks, H. B. Schlegel *et al.*, GAUSSIAN 03, Revision C.02 (Gaussian, Inc., Wallingford, CT, 2004).
[33] D. Gorse, D. Cavagnat, M. Pesquer, and C. Lapouge, J. Phys. Chem. **97**, 4262 (1993).
[34] T. Koopmans, Physica (Utrecht) **1**, 104 (1934).
[35] J. Cooper and R. N. Zare, J. Chem. Phys. **48**, 942 (1968).
[36] E. Surber, R. Mabbs, and A. Sanov, J. Phys. Chem. A **107**, 8215 (2003).
[37] C. M. Oana and A. I. Krylov, J. Chem. Phys. **127**, 234106 (2007).
[38] C. M. Oana and A. I. Krylov, J. Chem. Phys. **131**, 124114 (2009).
[39] A. Sanov and R. Mabbs, Int. Rev. Phys. Chem. **27**, 53 (2008).